Proceedings of the ASME 2022
International Design Engineering Technical Conferences &
Computers and Information in Engineering Conference
IDETC/CIE 2022
August 14-17, 2021, St. Louis, MO, USA

DETC2022-89619

OPTIMIZING INTENTIONAL ISLANDING DESIGN STRATEGIES FOR ENHANCED FAILURE RESILIENCE OF POWER SYSTEMS

Jiaxin Wu[1], Xin Chen[1], Jie Zhang[2]and Pingfeng Wang[1,*]

[1]Industrial and Enterprise Systems Engineering, University of Illinois Urbana-Champaign, Urbana, IL, USA
[2]Mechanical Engineering, University of Texas Dallas, Richardson, TX, USA

ABSTRACT

Establishing cleaner energy generation therefore improving the sustainability of power systems is a crucial task in this century. One of the key strategies being pursued is to shift the dependence on fossil fuel to renewable technologies such as wind, solar, and nuclear. However, with the increasing number of heterogeneous components included in the power system, the complexity of the hybrid energy system becomes more significant, which makes it prone to system failures. The complex system imposes a more stringent requirement of the contingency plan to enhance the overall system resilience against potential system disruptive events. Among different strategies to ensure a resilient system, intentional islanding is commonly applied in practical applications for power systems. In this study, we address the challenges of intentional islanding design considering high penetration of renewable energy sources, and develop a hierarchical clustering-based design method for optimized intentional islanding strategies at the transmission level of a power system. To incorporate the renewable generation that relies on the inverter technology, the frequency measurements are considered to represent the transient response and further used as embedded information in the clustering algorithm. And in the case study, the stabilized post-disruption performance of the modified IEEE-9 bus test system demonstrates the capability of the proposed method for resilience enhancement.

Keywords: Intentional Islanding, power systems, disruptive management, spectral clustering

1. INTRODUCTION

With the increases on both scale and complexity, interdependent critical infrastructures (ICIs), such as power systems or transportation networks, become more vulnerable towards disruptive events. Such vulnerability therefore drives the research efforts that could lead to robust and resilient ICIs. For instance, how to efficiently design a large-scale system that can resist potential external disruptions, or how can the decision-maker evaluate the uncertain dynamic behavior of the ICI undergoing different disruptive events? Also, for large-scale ICIs, mitigating the cascading effects after occurrences of disruptive events is a crucial task for attaining reliable system operations. To quantify the system's performance during disruption, or to comprehend the system's capability toward uncertain disruptive scenarios, researchers have adopted the term "resilience" from the ecology field [1]. Different from the terminology of system reliability, in which the time-dependent degraded system performance and the possibility of failure are studied, the resilience metric is utilized to complement the analysis of real-time system behavior. Based on the U.S. Department of Defense report, a resilient ICI should not only withstand impacts of disruptive events but also need to acquire the capability of self-healing from damages [2]. Thus, to realize a resilient ICI through design or operational management strategies, the stakeholders need to tackle challenges in three folds: (1) with the possibility of external or internal disruptions, how should the system proactively detect the occurrence of abnormalities; (2) how large is the bandwidth of the ICI for withstanding adversarial impacts; (3) how quick the ICI can self-recover to its nominal state [3].

Motivated by the challenges in the previously mentioned three aspects, different frameworks have been proposed to help the ICI to establish self-healing capability after system disruptions therefore achieve failure resilience. Here, we categorize the research efforts about engineering resilience based on the temporal stages of the proposed frameworks, i.e. before and after the disruptions. During the steady-state when the system operates under its nominal performance, it's important to obtain a universal analytic framework to assess the resilience level of ICIs, by considering the potential disruptive events [4, 5]. Moreover, researchers have proposed to use a probabilistic graphical

*Corresponding author: pingfeng@illinois.edu
DETC conf paper: version 1.26, May 16, 2022

model such as Bayesian Network to gauge the system resilience level dynamically with evolving system behavior [6, 7]. It is also beneficial to optimize the system resilience during the initial design stage, where various resilience enhancement methods can be considered: setting up a preventive or corrective maintenance schedule, establishing appropriate redundancies, or conducting proactive system health management [8–10]. Although comprehensive pre-disruption frameworks have been proposed to either quantify the resilience of ICIs or introduce methodologies to improve the system resilience in advance, how a system should behave after disruptions thus to preserve resilient performance is still unknown. And without an appropriate post-disruption guiding/response framework, cascading failures induced by severe disruptions are inevitable, especially in closely coupled power systems. As a result, it's required to study suitable recovery strategies to ensure system resilience after disruptions.

To tackle the challenges of achieving the self-healing capability of a resilient system, several real-time operational frameworks have been proposed to guide how the system should behave after disruptive events. For instance, researchers try to attain a resilient operational framework by incorporating optimal scheduling for repair tasks [11, 12], as well as repair resources [13] with uncertainties, forming self-sustainable microgrids [14], and guided recovery through control strategies [15]. All aforementioned studies focus on solving for the optimal decisions of how to utilize the existing resources or back-ups to recover the ICI thus mitigating the effects of disruptions, on the basis of having a contingency plan such as network reconfiguration beforehand. In other words, during the post disruption stage, the self-recovery capability is realized in two steps: appropriate emergency response e.g. system reconfiguration, followed by performing optimal restorations. One advantage of distinguishing between the contingency plan and optimal recovery is that the corresponding optimization problem is easier to solve due to the nature of decomposed subproblems. As a result, setting up a reliable system reconfiguration plan is vital for ensuring system resilience. In the power system field, the system reconfiguration is widely used as a contingency plan i.e. the intentional islanding strategy for a system undergoing disturbances to mitigate cascading effects [16–19] or to form robust microgrid operations [20–23].

To briefly review existing intentional islanding frameworks, for example, Esmaeilian et al. [24] have proposed a spectral clustering based intentional islanding strategy to regulate the systems after disruptions, considering the system power flow as the major performance criterion. Moreover, to mitigate the effect of the presumption on the number of islands after disruptions, Sanchez-Garcia et al. [25] have utilized the unsupervised hierarchical clustering technique to conduct the system partitioning. Dabbaghjamanesh et al. [26] have improved the robustness of the intentional islanding strategy by considering multiple electrical information embedded in the system along with the dynamic power flow measurement in the algorithm.

However, all aforementioned works have focused on power systems only with synchronous generators. As for modern power girds with large renewable penetration, the system performance will be largely influenced by the behaviour of the inverter-based generation. Hence, how to perform the intentional islanding operation for power systems with renewable penetration is still a crucial challenge for improving the overall system resilience. In this paper, we present an extended study for conducting the intentional islanding design for transmission level systems with renewable generations. The proposed framework utilizes the hierarchical spectral clustering technique based on both systems' static and dynamic information, and a case study with the modified IEEE-9 bus test network has been employed for the demonstration purpose.

The remaining parts of the paper is organized as follows: Sec. 2 introduces the proposed the intentional islanding methodology in detail, where the spectral graph clustering algorithm is coupled with the Grassmann manifold technique to accommodate the heterogeneous information extracted from the system. Sec. 3 presents a case study results based on the IEEE-9 bus test system to validate the proposed islanding design framework. And Sec. 4 summarizes the study along with discussion about future research directions.

2. CLUSTERING FOR INTENTIONAL ISLANDING

The intentional islanding is usually realized by conducting node clustering for the power system represented as a graph. As for the clustering methods, the K-Means algorithm is widely used for identifying inherent patterns of high dimensional data. The algorithm assumes that each sample point belongs exclusively to one latent cluster. And it assigns the data point X_j to the cluster S_i in terms of minimizing the overall Euclidean distance from the cluster center μ_i to each point. And the overall objective for a dataset with n samples can be expressed as:

$$\arg\min_{S} \sum_{i=1}^{n} \sum_{x_j \in S_i} ||X_j - \mu_i||^2. \tag{1}$$

Although the K-Means algorithm has adequate clustering performance for tabular data, it cannot be directly applied to graph-structured data, e.g., social networks and infrastructure networks. Since the Euclidean distance cannot directly reflect the difference between the nodes in the graphical system. To remedy this limitation of the K-Means algorithm, spectral graph theory can be incorporated. To be self-contained, we introduce the spectral clustering algorithm as well as the graphical information embedding mechanism for conducting intentional islanding in the following sections.

2.1 Spectral Graph Theory

Let a graph $\mathcal{G} = (\mathcal{V}, \mathcal{E})$ with vertex set $\mathcal{V}$ and edge set $\mathcal{E}$ represent the interconnected system. To be specific, for a N-bus power system, the corresponding graphical notation can be written as $\mathcal{V} := \{1, 2, \ldots, N\}$ and $\mathcal{E} := V \times V$. In the graph, the buses connecting to loads and generations are the vertices while the transmission lines are the edges. Moreover, based on the connection status between each pair of buses, a square connectivity matrix $W_{ij}^t \in \mathbb{R}^{V \times V}$ can be constructed as:

$$W_{ij}^t = \begin{cases} 1 & \text{if } (i,j) \in \mathcal{E}, \\ 0 & \text{otherwise.} \end{cases} \tag{2}$$

Notice that the W^t_{ij} is symmetric and follows the convention that all diagonal entries equal to zero, i.e., no self-loop. The connectivity matrix solely indicates the topological information of the graph-structured system. Besides the connectivity matrix, the power system requires other matrices to embed the electrical information it preserves, such as the power flow and resistance/reactance. Thus, by using W^t_{ij} as an analogy, matrices for the electrical properties are defined as:

$$W^p_{ij} = \begin{cases} \frac{|P_{ij}|+|P_{ji}|}{2} & \text{if } (i,j) \in \mathcal{E}, \\ 0 & \text{otherwise,} \end{cases} \tag{3}$$

where P_{ij} and P_{ji} are the active power flow on each transmission line considering the line loss. Notice that, uncertainties always arise in the hybrid energy system due to the renewable parts, for instance the wind turbines. In such a case, the stake holder can utilize the historical intraday power flow data to derive an accurate representation of W^P_{ij}. Besides the power flow information, the matrix for admittance of the system can be obtained as:

$$W^a_{ij} = \begin{cases} \frac{1}{\sqrt{R^2_{ij}+X^2_{ij}}} & \text{if } (i,j) \in \mathcal{E}, \\ 0 & \text{otherwise,} \end{cases} \tag{4}$$

where R_{ij} and X_{ij} are the resistance and reactance of the transmission lines, respectively. Similar to the connectivity matrix W^t_{ij}, the power flow matrix W^p_{ij} and admittance matrix W^a_{ij} are also symmetric with all diagonal entries being zeros.

The motivation of establishing the aforementioned three weight matrices is that they measure how strong a line connection would be when conducting intentional islanding by clustering nodes. In other words, disconnecting a transmission line with a large weight to form islands after clustering will lead to a large penalty in the objective of the clustering algorithm. And this behavior is desirable for intentional islanding to prevent cascading failures. Since buses directly connected are more likely to stay in the same cluster with similar operating conditions. Moreover, a larger admittance means a shorter electrical distance, and the buses connected by a transmission line with a small electrical distance should be in the same cluster after the islanding. Similarly, transmission lines carrying large power flow should not be cut and form isolated islands, which could lead to a large imbalance in load/generation and load shedding.

In order to cluster nodes based on introduced weight matrices and fulfill the intentional islanding task, we need to further derive the Laplacian matrix of the graph. The Laplacian matrix embeds the nodal information from the graph system into a pseudo-tabular form, which can be used later as the input to clustering algorithms developed based on structured data. And it is defined as $L = D - W$ where D is the degree matrix of the graph, The degree matrix is diagonal and can be obtained from $D = diag(\sum_j W_{ij})$. That is, the matrix D has all zeros on its non-diagonal entries, while the diagonal elements are the row sum of the weight matrix. In this way, each element of the Laplacian matrix has the form

$$L_{ij} = \begin{cases} d_i & \text{if } i = j, \\ -w_{ij} & \text{if } (i,j) \in \mathcal{E}, \\ 0 & \text{otherwise,} \end{cases} \tag{5}$$

where d_i is the degree of node i, i.e. the number of direct neighbors of each node. Usually, we will work on the normalized Laplacian matrix, which is scale independent and has better results for clustering. The normalized Laplacian matrix is calculated as $L_n = D^{1/2}LD^{-1/2}$. After normalization, the entries of the Laplacian matrix are

$$L_{n,ij} = \begin{cases} 1 & \text{if } i = j, \\ \frac{-w_{ij}}{\sqrt{d_i d_j}} & \text{if } (i,j) \in \mathcal{E}, \\ 0 & \text{otherwise.} \end{cases} \tag{6}$$

One characteristic of the Laplacian matrix is that it carries the spectral information of the graph. We can perform eigendecomposition on the Laplacian matrix and treat the eigenvectors as the spectral embeddings. Then by conducting clustering on these obtained spectral embeddings, we can discover the latent clusters for the graphical system. The overall roadmap of such a clustering technique is to use the first K eigenvectors of the Laplacian matrix as the geometric coordinates of the N data points defined in $\mathbb{R}^K$. Then these coordinates can be treated as in Euclidean space and be clustered by standard clustering techniques such as the K-Means algorithm. Notice that all spectra of the normalized graph Laplacian, i.e., its eigenvalues, always lie between zero and two, which is desirable when representing the nodal similarities by the corresponding eigenvectors.

2.2 Hierarchical Spectral Clustering

In Sec. 2.1, we have briefly introduced the spectral clustering algorithm for graph systems based on the K-Means algorithm. However, one drawback of the K-Means based spectral clustering is that the number of clusters, K, needs to be predefined. For intentional islanding to avoid cascading failures, the number of islands cannot be easily assumed beforehand but need to be determined based on the online operational condition. To overcome this limitation of the K-Means algorithm, this study utilizes hierarchical clustering on the spectral domain of the graph.

Different from the K-Means algorithm, which directly outputs the partitioning results based on the given number of clusters K and omits the inner connection between the nodes in the same cluster, the hierarchical clustering gives partitioning results with finer intra-cluster detail. The results of the hierarchical clustering are usually interpreted by the tree-like dendrogram, where each leaf is the individual node in the graph. The leaves of the dendrogram can also be viewed as clusters with a cardinality of one. And the goal of the clustering algorithm is to merge the closest clusters into a bigger cluster at each step following a bottom-up approach. To determine the best merging strategy, the Wade linkage criterion [27] is used as the metric in this study:

$$d(u,v) = \sqrt{\frac{|v|+|s|}{T}d(v,s)^2 + \frac{|v|+|t|}{T}d(v,t)^2 - \frac{|v|}{T}d(s,t)^2}, \tag{7}$$

where u is a merged cluster from subclusters s and t, v is a unused cluster in parallel with s and t, $|*|$ is the cardinality operator, and T equals the sum of $|s|$, $|t|$, and $|v|$. The Wade linkage criterion is a variance minimization metric and picks two clusters to form one that leads to the lowest sum of squared differences within

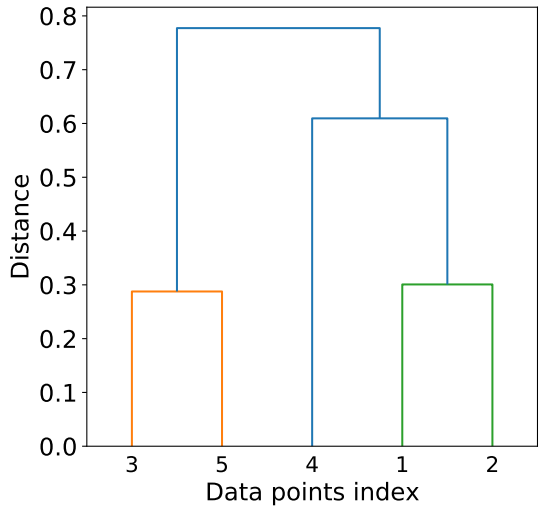

FIGURE 1: A sample dendrogram based on the result of the hierarchical clustering.

the clusters. This variance minimizing characteristic makes the Wade linkage criterion similar to the objective of the traditional K-Means algorithm, but in a hierarchical setting. Again, with the Wade linkage criterion, the goal is to merge two clusters providing the smallest $d(u, v)$ until all nodes are merged into the single cluster, which is the root of the dendrogram.

After performing the hierarchical clustering, the dendrogram of the clustering results can be derived. Figure 1 shows an example of the dendrogram. After a disruptive event, based on the specific system status, the number of clusters can be determined. And the clustering results can be obtained by cutting the dendrogram at the corresponding level. For instance, if three clusters are preferred for the clustering results shown in Fig. 1, then the islanding results can be obtained by cutting the tree at a level around $d = 0.6$ to have three clusters $\{3, 5\}$, $\{4\}$, and $\{1, 2\}$. The advantage of obtaining the tree-like results for clustering is that it reveals the finer structure of the system, compared to directly outputting the partitions by using the traditional K-Means algorithm. At various levels of the clustering resolution, the practitioner can zoom in or out to examine different structures of the clusters, and follow how each cluster is formed hierarchically.

2.3 Grassmann Manifold

The aforementioned study has not considered the multiple Laplacian matrix defined simultaneously for the graph. In [25], the authors demonstrate different intentional islanding results by using Laplacian matrices derived from different information, for instance, the average power flow and the admittance. But the scale of heterogeneous information embedded in the Laplacian matrix may be different, and it is required to normalize the magnitude to a unified scale before executing the clustering process. Thus, how to combine all different kinds of electrical information of the power system remains to be answered. Rather than treat different types of the Laplacian matrices separately as in [25], here we adopt the Grassmann manifold for multiple matrices in order to derive a unified Laplacian matrix for clustering.

A Grassmann manifold $G(K, N)$ can be defined as the set of K dimensional linear subspaces in $\mathbb{R}^N$, where each exclusive subspace is mapped to an exclusive point on the manifold. To find a unified Laplacian matrix, or the Grassmann manifold for a graph with M distinct Laplacian matrices, several steps need to be taken [28]:

1. Derive Laplacian matrix L_i for each graph G_i defined based on different weight matrices
2. Each G_i can be represented through the spectral embeddings matrix $U_i \in \mathbb{R}^{N\times K}$ from the first K eigenvectors of L_i
3. Each U_i can be considered as a K dimensional subspaces in $\mathbb{R}^N$
4. The main objective becomes combing these several subspaces by finding a typical subspace $span(U)$, which is closest to all the subspaces $span(U_i)$; this can be written as a minimization program:

$$\min_{U\in\mathbb{R}^{N\times K}} \sum_{i=1}^{M} tr(U^T L_i U) + \alpha \left[kM - \sum_{i=1}^{M} tr(UU^T U_i U_i^T) \right] \tag{8}$$

5. The solution of the above minimization problem is the unified Laplacian matrix for clustering:

$$L_{uni} = \sum_{i=1}^{M} L_i - \alpha \sum_{i=1}^{M} U_i U_i^T \tag{9}$$

2.4 Choose the Embedding Space

Once we have a unified Laplacian matrix derived from multiple heterogeneous Laplacian matrices as shown in Eqn. 9, then the intentional islanding can be achieved by performing hierarchical clustering on the Laplacian matrix as the spectral embedding of the graph.

Although we don't need to specify the number of clusters K beforehand to perform the hierarchical clustering, there is still a decision for choosing the subspace dimension K to embed the networked system. Without generator coherency, the number of desired dimensions K is unknown and can be problem-dependent. But one practical approach to make the optimal decision for the subspace dimension is to calculate the eigenvalues of the Laplacian matrix and derive the eigengap as a metric. The eigengap is the difference between the consecutive eigenvalues and can be found by

$$\gamma(\lambda_i) = |\lambda_{i+1} - \lambda_i|, \tag{10}$$

where λ_i is the i-th eigenvalue of the Laplacian matrix. And the normalized eigengap measured in percentage can be obtained from

$$\gamma_n(\lambda_i) = \frac{\gamma(\lambda_i)}{\lambda_{i+1}}. \tag{11}$$

After deriving the eigengaps, how to determine the optimal K remains to be discussed. Here we need to introduce the basic metric used to measure the quality of the intentional islanding without the electrical properties. Let's denote the volume of a cluster as $vol(A) = \sum_{i\in A, j\in A} W_{ij}$, where A is a subset of the vertices that

form the cluster. Based on the expression of the $Vol(A)$, one can see that it actually measures the closeness of the nodes inside the same cluster. Moreover, the boundary of the cluster is denoted as $b(A) = \sum_{i \in A, j \notin A} W_{ij}$, which measures the strength of interaction between the cluster and neighbors outside the cluster A. And the conductance $\Phi(A)$ of the cluster A can be defined as the quotient $\frac{b(A)}{vol(A)}$. For an effective clustering strategy, the goal is to partition the graph into clusters with the smallest conductance. In other words, the optimal islanding results should only include clusters that have strong interactions within the cluster and weak connections to the rest of the graph outside the cluster. Formally, this clustering task can be written as the k-way partitioning problem [29]. Multiple subsets of vertices, i.e., clusters, $A_1, \ldots, A_k$ are a k-way partition of the original graph $\mathcal{G}$ if $A_i \cap A_j = \emptyset$ for different i, j and $\cup_{i=1}^{k} A_i = \mathcal{V}$. The objective of the k-way partitioning problem can be defined by

$$\rho(k) := \min_{A_1,\ldots,A_k} \max_{1 \le i \le k} \Phi(A_i). \tag{12}$$

Following the definition of the objective, the partition tries to enforce that the conductance of any cluster A_i is at most the $\rho(k)$, i.e., the k-way expansion constant. Finding the optimal partition that optimizes the $\rho(k)$ is generally not computationally efficient for large-scale networks. Moreover, solving the k optimal cuts on a graph such as to search for the optimal solution of Eqn. 12 is usually NP-hard [30]. Nonetheless, the spectral clustering algorithm provides an approximation of the true optimum of the NP-hard problem. To be specific, Lee et al. [31] prove that performing spectral clustering on a graph G provides a bound for the k-way expansion constant, defined by higher-order Cheeger inequality:

$$\frac{\lambda_k}{2} \le \rho(k) \le O(k^2)\sqrt{\lambda_k}, \tag{13}$$

where $0 \le \lambda_1 \le \cdots \le \lambda_n \le 2$ are the sorted eigenvalues of the normalized Laplacian matrix of the original graph. Equation 13 suggests that a graph $\mathcal{G}$ can have good quality clusters if and only if the eigenvalue λ_k is small, which leads to a small k-way expansion constant. Nonetheless, the practical approach for choosing the optimal K is not only determined by the Cheeger inequality, which always gives the best result when choosing K to be one, and λ_1 is the smallest eigenvalue. In general, K is chosen to be the number associated with a large eigengap, and this approach has been proved by Lee et al. [31]. In their work they show that if there is significant gap between the eigenvalues of $\mathcal{G}$, then Eqn. 13 can be rewritten to be independent on K:

$$\max_{1 \le i \le k} \Phi(A_i) \le \sqrt{\lambda_k / \delta^3}, \tag{14}$$

where $\delta \in (0, \frac{1}{3})$, and λ_k is the k-th smallest eigenvalue of the graph Laplacian L. That is, after obtaining the eigengap results from Eqn. 11, we need to choose the K corresponding to a relatively large eigengap $\gamma_n(\lambda_k)$. This choice of K not only leads to a small graph expansion constant with a small eigenvalue, but also provides a reasonable number of dimensions for the spectral embedding.

2.5 Working with Renewables

All the Laplacian matrices defined in the previous sections are static and do not take the system's dynamic response into consideration. Moreover, the different behavior of the renewable generation is not covered. Thus in this section, how to derive the dynamic response of the renewable generation coupled in the power grid is discussed. In [32], the authors have analyzed the major factor for deriving the dynamic response of the renewable generation. Take a wind power plant (WPP) as an example: if the WPP capacity is large, then the point of common coupling (PCC) transient response will be dominated by converter dynamics. In this case, the WPP will operate as a separate electrical area because of the distinct behavior different from nearby synchronous generators. However, if the WPP capacity is relatively low, then the WPP transient response at PCC is imposed by the rest of the power system and the WPP dynamic response is coherent with other generators. As a result, the PCC dynamics can be used as a proxy to identify the coherence of the renewable with other components inside the grid. Thus, this study adopts a measurement-based method and utilizes frequency deviation signals from system nominal frequency to identify generator coherency with the presence of renewable generation. And the coherency is treated as another type of Laplacian matrix for the generator dynamic information in the clustering algorithm.

The frequency deviation signal at each bus i can be obtained by

$$\Delta f_{i,t+\Delta t} = \frac{1}{\omega_0}\left(\frac{\phi_{i,t+\Delta t} - \phi_{i,t}}{\Delta t}\right), \tag{15}$$

where ω_0 is the system nominal frequency, and ϕ_i is the voltage phase angle at bus i. With the temporal frequency deviation signals, the frequency deviation vector of bus i can be constructed from frequency deviation measurement at different time instants.

$$\Delta f_i = \left[\ldots, \Delta f_{i,t-\Delta t}, \Delta f_{i,t}, \Delta f_{i,t+\Delta t}, \ldots\right]^T. \tag{16}$$

Once the frequency deviation vector of each bus after the disruption is obtained, the coherency between each pair of buses can be measured by the coherency coefficient CC_{ij}, which is derived from the Cosine similarity of the corresponding frequency deviation vectors.

$$CC_{ij} = \frac{\Delta f_i \Delta f_j^T}{||\Delta f_i|| ||\Delta f_j||}. \tag{17}$$

Since we can derive the CC_{ij} for each pair of buses, or nodes in the graph, another weight matrix W_{ij}^f carrying dynamic information for the power system graph can be defined:

$$W_{ij}^f = \begin{cases} CC_{ij} & \text{if } (i,j) \in \mathcal{E} \\ 0 & \text{otherwise} \end{cases} \tag{18}$$

With all the above analysis, the overall road-map for conducting intentional islanding for power grids with renewable penetration can be summarized as:

1. Instead of finding the generator coherency first, use different information to define multi-layer graph Laplacian matrices for clustering

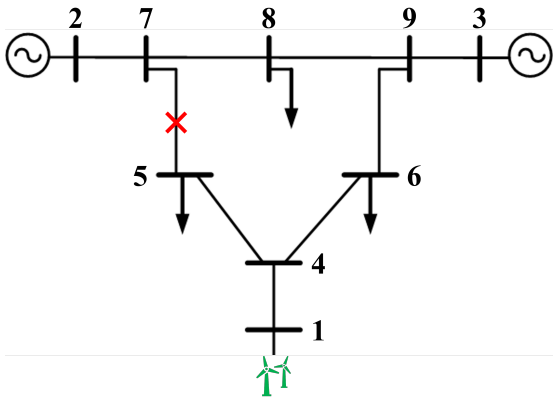

FIGURE 2: The one-line diagram of the IEEE-9 bus system, where the synchronous generator at bus 1 has been replaced by a wind farm (figure modified from [33]).

- Topology $w_{ij} = 1\ \forall ij \in \mathcal{E}$ measures the pure connectivity
- Admittance $w_{ij} = 1/\sqrt{R_{ij}^2 + X_{ij}^2}\ \forall ij \in \mathcal{E}$ measures the strength of connections (electrical distance)
- Average power flow $w_{ij} = (|P_{ij}| + |P_{ji}|)/2\ \forall ij \in \mathcal{E}$ measures the importance of a line during operation
- Frequency deviation $w_{ij} = CC_{ij}\ \forall ij \in \mathcal{E}$ measures the coherency of the buses, after a disruptive event

2. Construct the normalized Laplacian matrices and perform eigendecomposition. Analyze the eigengaps to determine the best number of embedding space K, for deriving the Grassmann manifold

3. Use the Grassmann manifold to derive a unified Laplacian based on the multi-layer information:

$$L_{uni} = \sum_{i=1}^{M} L_i - \alpha \sum_{i=1}^{M} U_i U_i^T$$

4. Conduct hierarchical clustering with connectivity constraints on the unified Laplacian

3. RESULTS OF CASE STUDIES

To validate the proposed clustering-based intentional islanding strategy, the IEEE 9-bus test systems is used for simulations. The data of the system can be found at [34]. We have modified the original test networks to include additional renewable generation, such as wind farms, to show the applicability of the intentional islanding for transmission networks with renewable generation. The simulation of the system dynamic response after disruptions within 20 seconds is conducted in the Power System Analysis Toolbox (PSAT) [35]. This study uses the 20 seconds span to represent the time window for the emergency response after disturbance. And line outages are simulated to happen at 1.5 second. Notice that, this study also conducts case studies based on a larger scale IEEE 118-bus system to test the performance of the proposed method on more practical applications.

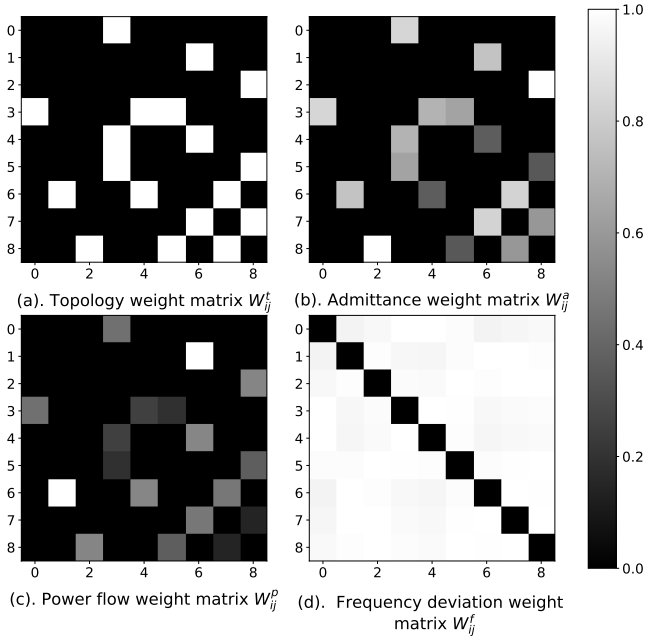

FIGURE 3: Four weight matrices constructed from the measurement data of the IEEE 9-bus system.

But due to space limitations, only the results of the 9-bus system are reported. Interested reader can refer to [36] for the complete experimental results.

Firstly, to demonstrate the major ideas and steps of the proposed intentional islanding strategy, we use the IEEE-9 bus system as the baseline model to illustrate the details of the main steps of the algorithm. Figure 2 shows the original layout of the IEEE 9-bus test case. The line outage happens at the transmission line $(7, 5)$, in which the network has disconnected afterward. To incorporate the renewable generation, the synchronous generator at bus 1 has been replaced by a wind farm. The capacity of the wind power generation is set to be 100 MVA and consists of 30 wind turbines. And this renewable generation corresponds to 33.3% of the total power generation in the system. The original IEEE-9 bus system has a special characteristic that all three synchronous generators in the system have different operating modes, even before adding the renewable generation. Thus, this observation indicates that these three generators connecting at bus 1, 2, and 3 need to be partitioned into separate islands with an effective intentional islanding strategy after disruptions. And because of this characteristic, studies about intentional islanding algorithms usually use the 9-bus system as the baseline model.

As discussed in Sec. 2.5, the first step for the clustering-based intentional islanding is to define the weight matrices for the system from different types of measurements. For the IEEE 9-bus system, four weight matrices are constructed as shown in Fig. 3. The indices of the weight matrices start from 0 following the 0-indexed convention of the coding language. From the matrices' data, it can be seen that except for the frequency deviation matrix, all other three matrices are sparse and share the same structure. This is due to the nature of connectivity: the power flow and the admittance can only be non-zero if there is a line between two

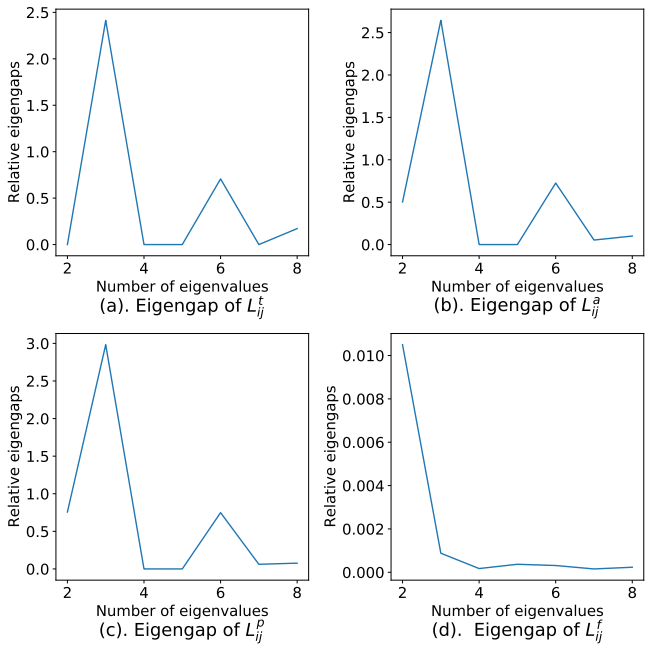

FIGURE 4: The eigengap obtained from the four Laplacian matrices defined based on topology, admittance, power flow, and frequency deviation

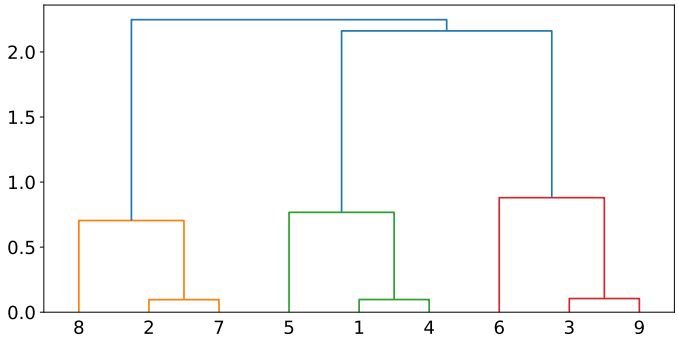

FIGURE 5: The dendrogram result of the hierarchical clustering for IEEE 9-bus system

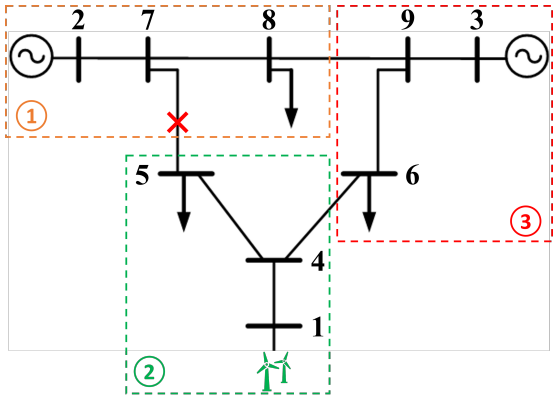

FIGURE 6: The intentional islanding results for the IEEE 9-bus system based on the derived dendrogram (figure modified from [33])

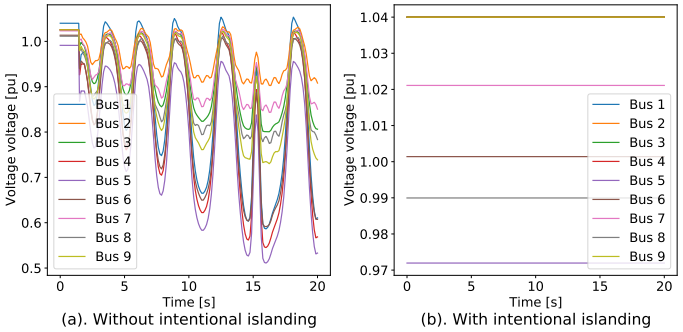

FIGURE 7: The dynamic response of the voltage magnitude at all buses of the IEEE 9-bus system after disruptions, with and without the intentional islanding operation

buses. And a power system is indeed a sparse graph, where the number of edges has the same scale as the number of nodes, i.e., $|\mathcal{E}| \propto |\mathcal{V}|$. In contrast, the frequency deviation matrix is obtained from the measurement of the dynamic system response. And the deviation is a pairwise relation between buses regardless of the connectivity of the system. Figure 3 shows that the frequency deviation matrix W_{ij}^{f} has much more non-zero entries compared to the topology, admittance, and power flow matrices. Thus, applying the Grassmann manifold to obtain a unified spectral embedding is a crucial task to conduct clustering because of the heterogeneous weight matrices.

Yet to derive the Grassmann manifold of the Laplacian matrices based on the weight matrices introduced above, we first need to determine the number of dimensions K of the spectral embedding. As discussed in Sec. 2.3, K is determined to be the number of i, which gives a large eigengap between two consecutive eigenvalues of the Laplacian matrix L. Thus Fig. 4 shows the eigengap results of the Laplacian matrix of the IEEE 9-bus system. Notice that the X-axis starts from the second eigenvalue since the smallest eigenvalue of any valid Laplacian matrix is always zero. Hence, from the plot, K is chosen to be three in order to obtain the K dimensional spectral embedding in the subspace for deriving the unified Laplacian matrix.

Figure 5 demonstrates the clustering result of the IEEE 9-bus system. After a disruption, the system operator can obtain an appropriate intentional islanding strategy based on the dendrogram. For example, if three islands are desired, then three clusters can be formed by cutting the tree at around 1.0 along the y-axis in the dendrogram. And the corresponding three clusters are the sub-trees that consist of buses $\{6, 5, 1, 4\}$, $\{3, 9\}$, and $\{8, 2, 7\}$. Figure 6 illustrates the IEEE 9-bus system after forming isolated islands.

To analyze the system dynamic response after the disruption with and without intentional islanding strategy, Fig. 7 and Fig. 8 summarize the transient voltage magnitude and voltage angle measurements for the IEEE-9 bus test network, respectively. When the system undergoes a line outage without intentional islanding, Fig. 7 shows that the voltage magnitudes of all buses deteriorate from the nominal state to unstable cyclical patterns swinging between 0.5 and 1.0 pu. And the oscillations become more significant as the simulation goes on: a cascading failure is

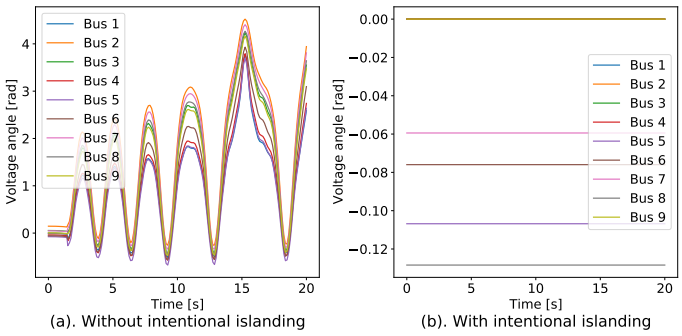

FIGURE 8: The dynamic response of the voltage angle at all buses of the IEEE 9-bus system after disruptions, with and without the intentional islanding operation

eventual for the system without any contingency plan. In comparison, with intentional islanding, the voltage measurements of all buses stay at steady states around 1.0 pu even with the presence of the disruptive event. This is due to the fact that multiple lines, including the damaged line, are actively disconnected to enforce the system forming isolated sub-systems. And each sub-system is powered by one generator solely to ensure that the frequency is consistent across the buses inside the same island. Moreover, Fig. 8 suggests that the voltage angle of each bus has the same trend as the voltage magnitude, which reveals the same benefit of having the clustering-based intentional islanding as a contingency plan toward disruptions.

4. CONCLUSION

To address the challenges of transmission system reliability along with the increasing level of renewable penetration, this study proposes a hierarchical clustering-based intentional islanding framework to guide the system transient operations after disruptions. Multiple layers of system real-time measurement data are considered including topology, electrical distance, as well as frequency deviation. To benefit from the heterogeneous information representing different aspects, this study adopts the Grassmann manifold algorithm to derive a unified embedding matrix for the final clustering. Moreover, because of the flexibility of the hierarchical clustering, the islanding decisions, i.e., the number of clusters formed, can be adjusted based on the stakeholders' prior knowledge. Also, to validate the proposed framework, the transient responses of the IEEE 9-bus test system after disruptions have been studied. However, in this study, we have only considered case studies with limited types of renewable generation, e.g., the wind farms with a relatively low level of penetration. In future studies, test systems with different types of generations are planned to be included, for instance, nuclear power plants with large generation capacities.

ACKNOWLEDGMENTS

This research is partially supported by the National Science Foundation through the Engineering Research Center for Power Optimization of Electro-Thermal Systems (POETS) with cooperative agreement EEC-1449548, and the U.S. Department of Energy's Office of Nuclear Energy under Award No. DE-NE0008899.

REFERENCES

[1] DeAngelis, D. L. "Energy Flow, Nutrient Cycling, and Ecosystem Resilience." *Ecology* Vol. 61 No. 4 (1980): pp. 764–771. DOI 10.2307/1936746.

[2] Goerger, Simon R., Madni, Azad M. and Eslinger, Owen J. "Engineered resilient systems: A DoD perspective." *Procedia Computer Science*, Vol. 28: pp. 865–872. 2014. DOI 10.1016/j.procs.2014.03.103.

[3] Walker, Brian, Holling, C. S., Carpenter, Stephen R. and Kinzig, Ann. "Resilience, adaptability and transformability in social-ecological systems." *Ecology and Society* Vol. 9 No. 2. DOI 10.5751/ES-00650-090205.

[4] Yodo, Nita and Wang, Pingfeng. "Engineering Resilience Quantification and System Design Implications: A Literature Survey." *Journal of Mechanical Design* Vol. 138 No. 11. DOI 10.1115/1.4034223. 111408.

[5] Sharma, Neetesh, Tabandeh, Armin and Gardoni, Paolo. "Resilience analysis: a mathematical formulation to model resilience of engineering systems." *Sustainable and Resilient Infrastructure* Vol. 3 No. 2 (2018): pp. 49–67. DOI 10.1080/23789689.2017.1345257.

[6] Yodo, Nita and Wang, Pingfeng. "Resilience modeling and quantification for engineered systems using Bayesian networks." *Journal of Mechanical Design* Vol. 138 No. 3.

[7] Yodo, Nita, Wang, Pingfeng and Zhou, Zhi. "Predictive Resilience Analysis of Complex Systems Using Dynamic Bayesian Networks." *IEEE Transactions on Reliability* Vol. 66 No. 3 (2017): pp. 761–770. DOI 10.1109/TR.2017.2722471.

[8] Compare, Michele and Zio, Enrico. "Predictive Maintenance by Risk Sensitive Particle Filtering." *IEEE Transactions on Reliability* Vol. 63 No. 1 (2014): pp. 134–143. DOI 10.1109/TR.2014.2299651.

[9] Yodo, Nita and Wang, Pingfeng. "A control-guided failure restoration framework for the design of resilient engineering systems." *Reliability Engineering System Safety* Vol. 178 (2018): pp. 179–190. DOI https://doi.org/10.1016/j.ress.2018.05.018.

[10] Yodo, Nita, Wang, Pingfeng and Rafi, Melvin. "Enabling Resilience of Complex Engineered Systems Using Control Theory." *IEEE Transactions on Reliability* Vol. 67 No. 1 (2018): pp. 53–65. DOI 10.1109/TR.2017.2746754.

[11] Ouyang, Min and Fang, Yiping. "A Mathematical Framework to Optimize Critical Infrastructure Resilience against Intentional Attacks." *Computer-Aided Civil and Infrastructure Engineering* Vol. 32 No. 11 (2017): pp. 909–929. DOI 10.1111/mice.12252.

[12] Wu, Jiaxin and Wang, Pingfeng. "Risk-averse optimization for resilience enhancement of complex engineering systems under uncertainties." *Reliability Engineering & System Safety* Vol. 215 (2021): p. 107836. DOI https://doi.org/10.1016/j.ress.2021.107836. URL https://www.sciencedirect.com/science/article/pii/S0951832021003562.

[13] Wu, Jiaxin and Wang, Pingfeng. "Post-disruption performance recovery to enhance resilience of interconnected network systems." *Sustainable and Resilient Infrastructure* Vol. 6 No. 1-2 (2021): pp. 107–123.

[14] Chen, Chen, Wang, Jianhui, Qiu, Feng and Zhao, Dongbo. "Resilient Distribution System by Microgrids Formation after Natural Disasters." *IEEE Transactions on Smart Grid* Vol. 7 No. 2 (2016): pp. 958–966. DOI 10.1109/TSG.2015.2429653.

[15] Wu, Jiaxin and Wang, Pingfeng. "A comparison of control strategies for disruption management in engineering design for resilience." *ASCE-ASME Journal of Risk and Uncertainty in Engineering Systems, Part B: Mechanical Engineering* Vol. 5 No. 2. DOI 10.1115/1.4042829.

[16] Baran, M.E. and Wu, F.F. "Network reconfiguration in distribution systems for loss reduction and load balancing." *IEEE Transactions on Power Delivery* Vol. 4 No. 2 (1989): pp. 1401–1407. DOI 10.1109/61.25627.

[17] Guedes, Lucas S. M., Lisboa, Adriano C., Vieira, Douglas A. G. and Saldanha, Rodney R. "A Multiobjective Heuristic for Reconfiguration of the Electrical Radial Network." *IEEE Transactions on Power Delivery* Vol. 28 No. 1 (2013): pp. 311–319. DOI 10.1109/TPWRD.2012.2218260.

[18] Dall'Anese, Emiliano and Giannakis, Georgios B. "Sparsity-Leveraging Reconfiguration of Smart Distribution Systems." *IEEE Transactions on Power Delivery* Vol. 29 No. 3 (2014): pp. 1417–1426. DOI 10.1109/TPWRD.2014.2302912.

[19] Conti, Stefania and Rizzo, Santi Agatino. "Monte Carlo Simulation by Using a Systematic Approach to Assess Distribution System Reliability Considering Intentional Islanding." *IEEE Transactions on Power Delivery* Vol. 30 No. 1 (2015): pp. 64–73. DOI 10.1109/TPWRD.2014.2329535.

[20] Soni, Nimish, Doolla, Suryanarayana and Chandorkar, Mukul C. "Improvement of Transient Response in Microgrids Using Virtual Inertia." *IEEE Transactions on Power Delivery* Vol. 28 No. 3 (2013): pp. 1830–1838. DOI 10.1109/TPWRD.2013.2264738.

[21] Elrayyah, Ali, Sozer, Yilmaz and Elbuluk, Malik E. "A Novel Load-Flow Analysis for Stable and Optimized Microgrid Operation." *IEEE Transactions on Power Delivery* Vol. 29 No. 4 (2014): pp. 1709–1717. DOI 10.1109/TPWRD.2014.2307279.

[22] Ambia, Mir Nahidul, Meng, Ke, Xiao, Weidong and Dong, Zhao Yang. "Nested Formation Approach for Networked Microgrid Self-Healing in Islanded Mode." *IEEE Transactions on Power Delivery* Vol. 36 No. 1 (2021): pp. 452–464. DOI 10.1109/TPWRD.2020.2977769.

[23] Azizi, Resul and Seker, Serhat. "Microgrid Fault Detection and Classification Based on the Boosting Ensemble Method with the Hilbert-Huang Transform." *IEEE Transactions on Power Delivery* (2021): pp. 1–1DOI 10.1109/TPWRD.2021.3109023.

[24] Esmaeilian, Ahad and Kezunovic, Mladen. "Prevention of power grid blackouts using intentional islanding scheme." *IEEE Transactions on Industry Applications* Vol. 53 No. 1 (2017): pp. 622–629. DOI 10.1109/TIA.2016.2614772.

[25] Sánchez-García, Rubén J., Fennelly, Max, Norris, Sean, Wright, Nick, Niblo, Graham, Brodzki, Jacek and Bialek, Janusz W. "Hierarchical spectral clustering of power grids." *IEEE Transactions on Power Systems* Vol. 29 No. 5 (2014): pp. 2229–2237. DOI 10.1109/TPWRS.2014.2306756.

[26] Dabbaghjamanesh, Morteza, Wang, Boyu, Kavousi-Fard, Abdollah, Mehraeen, Shahab, Hatziargyriou, Nikos D., Trakas, Dimitris N. and Ferdowsi, Farzad. "A Novel Two-Stage Multi-Layer Constrained Spectral Clustering Strategy for Intentional Islanding of Power Grids." *IEEE Transactions on Power Delivery* Vol. 35 No. 2 (2020): pp. 560–570. DOI 10.1109/TPWRD.2019.2915342.

[27] de Amorim, Renato Cordeiro. "Feature relevance in ward's hierarchical clustering using the L p norm." *Journal of Classification* Vol. 32 No. 1 (2015): pp. 46–62.

[28] Dong, Xiaowen, Frossard, Pascal, Vandergheynst, Pierre and Nefedov, Nikolai. "Clustering on multi-layer graphs via subspace analysis on Grassmann manifolds." *2013 IEEE Global Conference on Signal and Information Processing, GlobalSIP 2013 - Proceedings*: pp. 993–996. 2013. DOI 10.1109/GlobalSIP.2013.6737060.

[29] Peng, Richard, Sun, He and Zanetti, Luca. "Partitioning well-clustered graphs: Spectral clustering works!" *SIAM Journal on Computing* Vol. 46 No. 2 (2017): pp. 710–743. DOI 10.1137/15M1047209. URL 1411.2021.

[30] Garey, M. R., Johnson, D. S. and Stockmeyer, L. "Some simplified NP-complete graph problems." *Theoretical Computer Science* Vol. 1 No. 3 (1976): pp. 237–267. DOI 10.1016/0304-3975(76)90059-1.

[31] Lee, James R., Oveis Gharan, Shayan and Trevisan, Luca. "Multi-way spectral partitioning and higher-order cheeger inequalities." *Proceedings of the Annual ACM Symposium on Theory of Computing*: pp. 1117–1130. 2012. DOI 10.1145/2213977.2214078. URL 1111.1055.

[32] Khalil, Ahmed Mostafa and Iravani, Reza. "Power System Coherency Identification under High Depth of Penetration of Wind Power." *IEEE Transactions on Power Systems* Vol. 33 No. 5 (2018): pp. 5401–5409. DOI 10.1109/TPWRS.2018.2809548.

[33] Song, Yue, Hill, David J and Liu, Tao. "Small-disturbance angle stability analysis of microgrids: A graph theory viewpoint." *2015 IEEE Conference on Control Applications (CCA)*: pp. 201–206. 2015. IEEE.

[34] "WSCC 9-Bus System." https://icseg.iti.illinois.edu/wscc-9-bus-system/. Accessed: 2022-05-08.

[35] Milano, Federico. "An open source power system analysis toolbox." *IEEE Transactions on Power Systems* Vol. 20 No. 3 (2005): pp. 1199–1206. DOI 10.1109/TPWRS.2005.851911.

[36] Wu, Jiaxin, Chen, Xin, Badakhshan, Sobhan, Zhang, Jie and Wang, Pingfeng. "Spectral Graph Clustering for Intentional Islanding Operations in Resilient Hybrid Energy Systems." *arXiv preprint arXiv:2203.06579* .